

Status of theory for heavy muonic atoms

Natalia S. Oreshkina

Max Planck Institute for Nuclear Physics (Heidelberg)

Kaonic, Antiprotonic, Muonic, Pionic and “onia” exotic Atoms:
Interchanging knowledge and recent results
September 30, 2024



MAX-PLANCK-GESELLSCHAFT



Muons and Exotic Atoms

muon:

- similar properties as electron
 $q_e = q_\mu$
- much bigger mass
 $m_\mu \approx 207 m_e$
- “heavy electron”
- lifetime free muon $\approx 2\mu s$

→ β -decay:

- lives long enough to form bound states with other particles

Standard Model of Elementary Particles

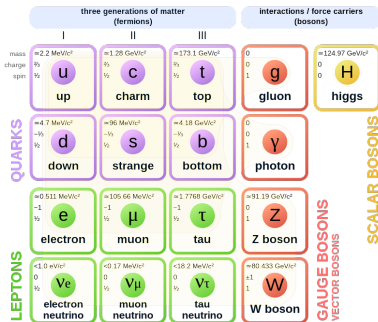
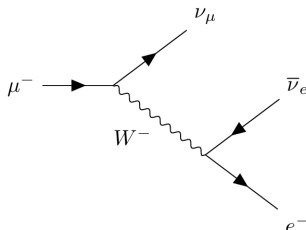


Fig: Wikipedia



Exotic atomic systems with muons

Hydrogenlike Atom



Muonium



Muonic Atom



Literature eg.:

- J. M. Bailey et al., Phys. Rev. A 3, 871 (1971)
- C. J. Oram et al., Phys. Rev. Lett. 52, 910 (1984)
- K. S. Khaw et al., Phys. Rev. A 94, 022716 (2016)

Exotic atomic systems with muons

Hydrogenlike Atom



Muonium



Muonic Atom



Literature eg.:

- J. M. Bailey et al., Phys. Rev. A 3, 871 (1971)
- C. J. Oram et al., Phys. Rev. Lett. 52, 910 (1984)
- K. S. Khaw et al., Phys. Rev. A 94, 022716 (2016)

exotic atoms with muons

- electromagnetically bound states
- reduce (muonium) or increase (muonic atom) nuclear structure effects

Muonic atoms' importance

Atomic Data and Nuclear Data Tables 99 (2013) 69–95



Contents lists available at SciVerse ScienceDirect

Atomic Data and Nuclear Data Tables

journal homepage: www.elsevier.com/locate/adt



Table of experimental nuclear ground state charge radii: An update

I. Angeli^a, K.P. Marinova^{b,*}

^a Institute of Experimental Physics, University of Debrecen, H-4010 Debrecen Pf. 105, Hungary

^b Joint Institute for Nuclear Research, 141980 Dubna, Moscow Region, Russia

ARTICLE INFO

Article history:

Received 9 August 2011

Received in revised form

10 November 2011

Accepted 2 December 2011

Available online 12 December 2012

Keywords:

Nuclear charge radii

Radii changes

Optical isotope shifts

K_{α} , X-ray isotope shifts

Electron scattering

Muonic atom spectra

ABSTRACT

The present table contains experimental root-mean-square (*rms*) nuclear charge radii R obtained by combined analysis of two types of experimental data: (i) radii changes determined from optical and, to a lesser extent, K_{α} X-ray isotope shifts and (ii) absolute radii measured by muonic spectra and electronic scattering experiments. The table combines the results of two working groups, using respectively two different methods of evaluation, published in ADNDT earlier. It presents an updated set of *rms* charge radii for 909 isotopes of 92 elements from ${}_1^H$ to ${}_{96}^{Cm}$ together, when available, with the radii changes from optical isotope shifts. Compared with the last published tables of R -values from 2004 (799 ground states), many new data are added due to progress recently achieved by laser spectroscopy up to early 2011. The radii changes in isotopic chains for He, Li, Be, Ne, Sc, Mn, Y, Nb, Bi have been first obtained in the last years and several isotopic sequences have been recently extended to regions far off stability, (e.g., Ar, Mo, Sn, Te, Pb, Po).

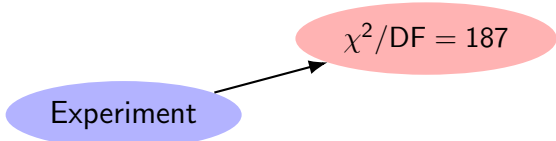
© 2012 Elsevier Inc. All rights reserved.

One of the best: ^{208}Pb

Experiment

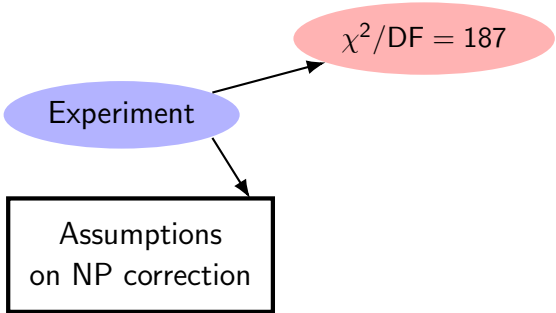
[1] Bergem *et al.*, PRC **37**, 2821 (1988)

One of the best: ^{208}Pb



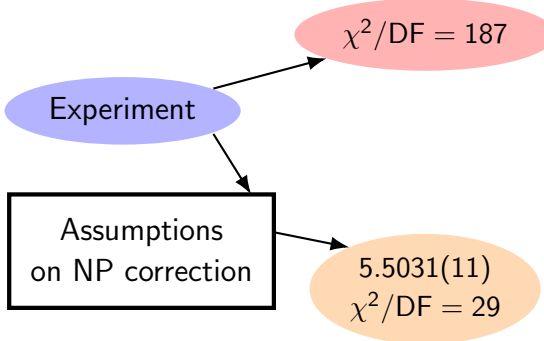
[1] Bergem *et al.*, PRC **37**, 2821 (1988)

One of the best: ^{208}Pb



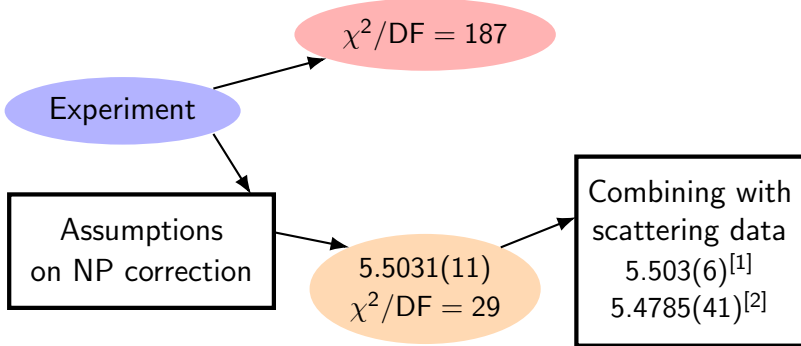
[1] Bergem *et al.*, PRC **37**, 2821 (1988)

One of the best: ^{208}Pb



[1] Bergem *et al.*, PRC **37**, 2821 (1988)

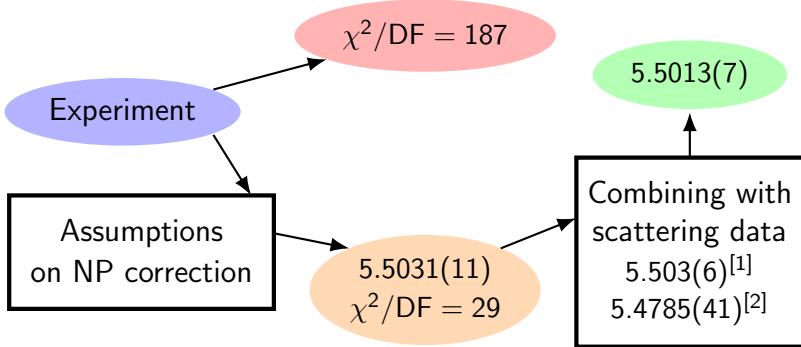
One of the best: ^{208}Pb



[1] Bergem *et al.*, PRC **37**, 2821 (1988)

[2] Fricke and Bernhardt, At. Data Nucl. Data Tables **60**, 177 (1995)

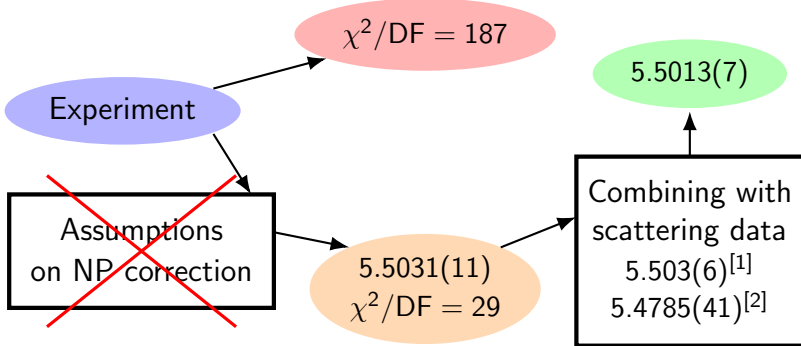
One of the best: ^{208}Pb



[1] Bergem *et al.*, PRC **37**, 2821 (1988)

[2] Fricke and Bernhardt, At. Data Nucl. Data Tables **60**, 177 (1995)

One of the best: ^{208}Pb

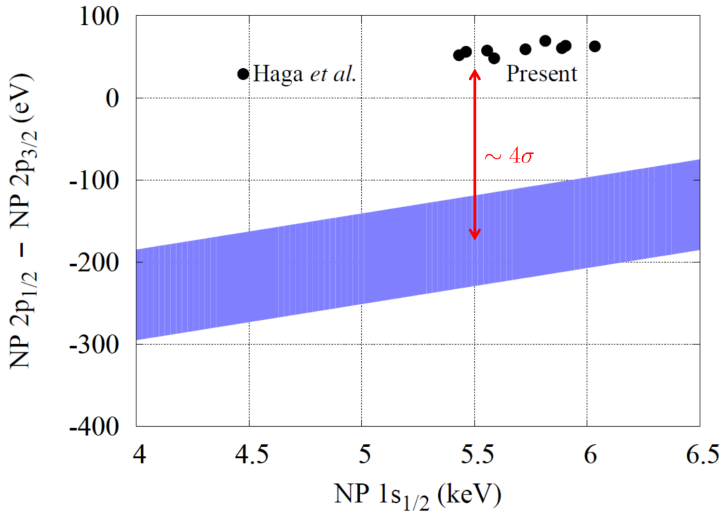


[1] Bergem *et al.*, PRC **37**, 2821 (1988)

[2] Fricke and Bernhardt, At. Data Nucl. Data Tables **60**, 177 (1995)

[3] Valuev *et al.*, PRL **128** 203001 (2022)

Nuclear polarization correction ^{208}Pb



around 150 eV, or 4σ standard deviations gap

Motivation to muon physics



Heavy muonic atoms spectroscopy at PSI

Outline

Introduction and Motivation

Very basic theory

Latest improvements

Results

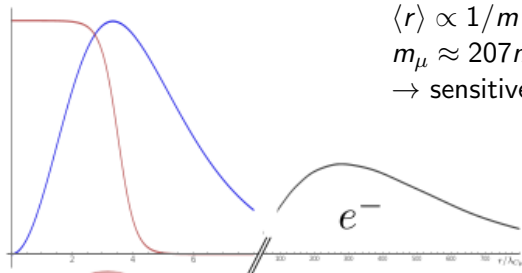
Summary



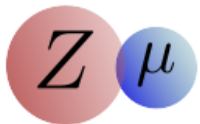
“Live fast, die young!”

<https://www.particlezoo.net>

Very basic theory



$\langle r \rangle \propto 1/m$
 $m_\mu \approx 207 m_e$
→ sensitive to nuclear structure

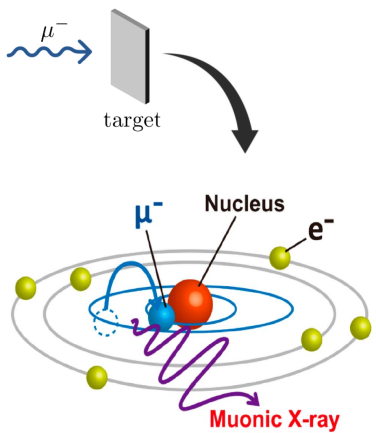


fit calculated spectra to
measured ones
→ determine nuclear parameters

Fig: Niklas Michel

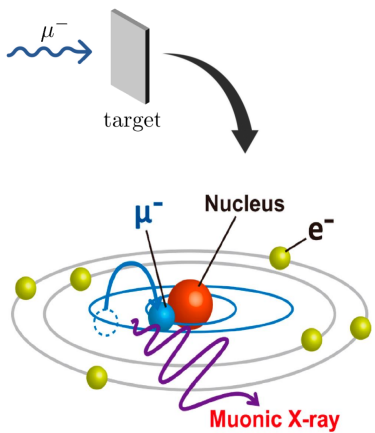
Access to muonic atoms

- capture and cascade:
 $10^{-12} - 10^{-9}$ s



<http://www.mdpi.com/2412-382-X/1/1/11/htm>

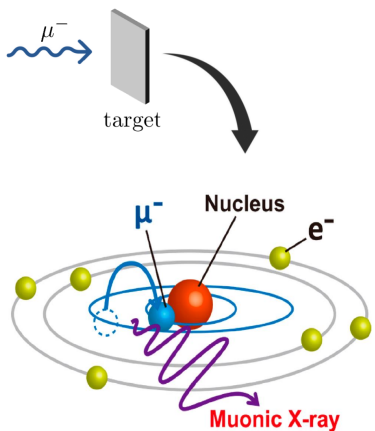
Access to muonic atoms



- capture and cascade: $10^{-12} - 10^{-9}$ s
- lifetime: $0.1 - 2.2 \mu\text{s}$
- always H-like

<http://www.mdpi.com/2412-382-X/1/1/11/htm>

Access to muonic atoms



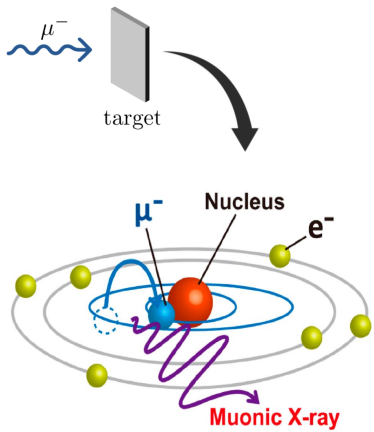
- capture and cascade:
 $10^{-12} - 10^{-9}$ s
- lifetime:
 $0.1 - 2.2 \mu\text{s}$
- always H-like
- decay channels

$$\mu^- \rightarrow e^- + \bar{\nu}_e + \nu_\mu$$

$$\mu^- + p \rightarrow n + \nu_\mu$$

<http://www.mdpi.com/2412-382-X/1/1/11/htm>

Access to muonic atoms

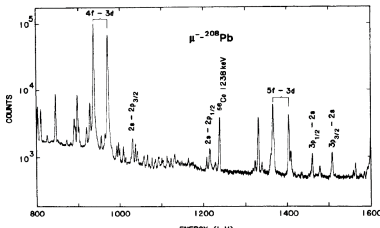


<http://www.mdpi.com/2412-382-X/1/1/11/htm>

- capture and cascade: $10^{-12} - 10^{-9}$ s
- lifetime: $0.1 - 2.2 \mu\text{s}$
- always H-like
- decay channels

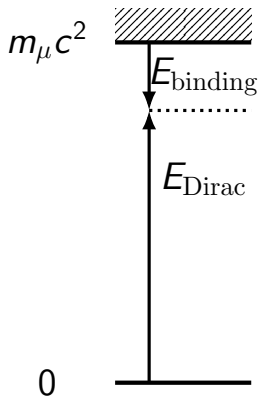
$$\mu^- \rightarrow e^- + \bar{\nu}_e + \nu_\mu$$

$$\mu^- + p \rightarrow n + \nu_\mu$$



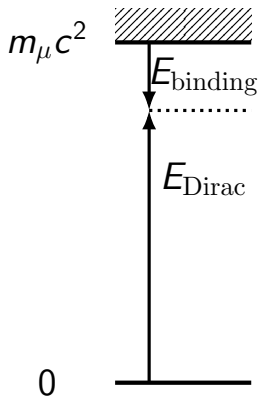
Dirac value and nuclear size

- Muons are close to the nucleus,
relativistic \rightarrow Dirac equation



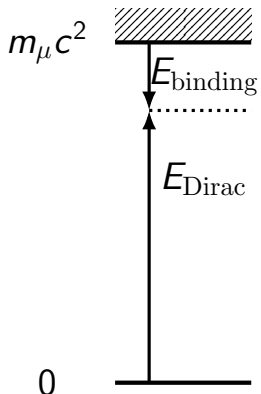
Dirac value and nuclear size

- Muons are close to the nucleus, relativistic \rightarrow Dirac equation



- $m_\mu c^2 \approx 100 \text{ MeV}$
 $E_{\text{Dirac}} \approx 80 \text{ MeV}$
 $E_{\text{binding}} \approx 20 \text{ MeV}$

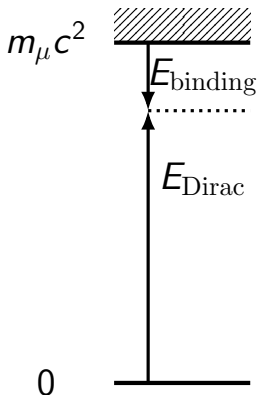
Dirac value and nuclear size



- Muons are close to the nucleus, relativistic \rightarrow Dirac equation
- $m_\mu c^2 \approx 100 \text{ MeV}$
 $E_{\text{Dirac}} \approx 80 \text{ MeV}$
 $E_{\text{binding}} \approx 20 \text{ MeV}$
- Extended nucleus: sphere,

$$V_{\text{Sph}}(r) = \begin{cases} a + br^2; & r \leq R \\ -\frac{Z\alpha}{r}; & r \geq R \end{cases}$$

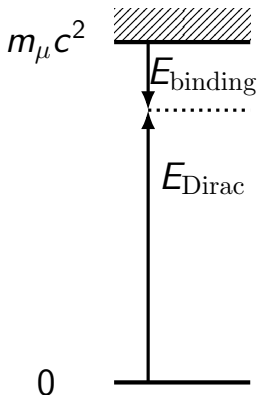
Dirac value and nuclear size



- Muons are close to the nucleus,
relativistic \rightarrow Dirac equation
- $m_\mu c^2 \approx 100 \text{ MeV}$
 $E_{\text{Dirac}} \approx 80 \text{ MeV}$
 $E_{\text{binding}} \approx 20 \text{ MeV}$
- Extended nucleus: sphere,
Fermi,

$$\rho_{a,c}^F(r_\mu) = \frac{N}{1 + e^{(r-c)/a}}$$

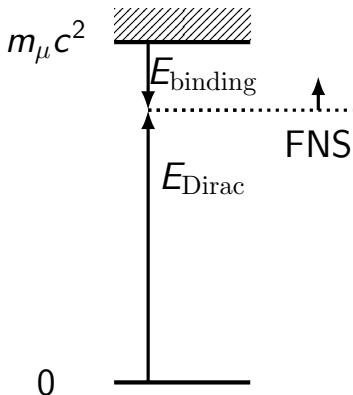
Dirac value and nuclear size



- Muons are close to the nucleus, relativistic → Dirac equation
- $m_\mu c^2 \approx 100 \text{ MeV}$
 $E_{\text{Dirac}} \approx 80 \text{ MeV}$
 $E_{\text{binding}} \approx 20 \text{ MeV}$
- Extended nucleus: sphere, Fermi, deformed Fermi

$$\rho_{a,c,\beta}(r_\mu, \vartheta_\mu) = \frac{N}{1 + e^{[r - c(1 + \beta Y_{20}(\vartheta_\mu))] / a}}$$

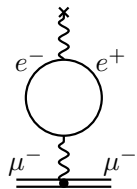
Dirac value and nuclear size



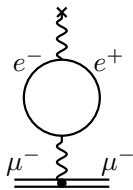
- Muons are close to the nucleus, relativistic → Dirac equation
- $m_\mu c^2 \approx 100 \text{ MeV}$
 $E_{\text{Dirac}} \approx 80 \text{ MeV}$
 $E_{\text{binding}} \approx 20 \text{ MeV}$
- Extended nucleus: sphere, Fermi, deformed Fermi
- $\Delta E_{\text{FNS}} \approx 10 \text{ MeV}$

$$\rho_{a,c,\beta}(r_\mu, \vartheta_\mu) = \frac{N}{1 + e^{[r - c(1 + \beta Y_{20}(\vartheta_\mu))] / a}}$$

Leading QED: Uehling

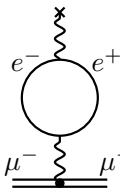


Leading QED: Uehling



$$V_{\text{Ue}}(r) = -\frac{2\alpha Z\alpha}{3r} \int_0^\infty dr' r' \rho(r') \left[\chi_2(2|r-r'|) - \chi_2(2|r+r'|) \right]$$

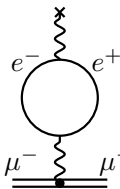
Leading QED: Uehling



$$V_{\text{Ue}}(r) = -\frac{2\alpha Z\alpha}{3r} \int_0^\infty dr' r' \rho(r') \left[\chi_2(2|r-r'|) - \chi_2(2|r+r'|) \right]$$

$$\chi_n(z) = \int_1^\infty dt \exp(-tz) \frac{1}{t^n} \left(1 + \frac{1}{2t^2} \right) \sqrt{1 - \frac{1}{t^2}}$$

Leading QED: Uehling

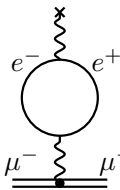


$$V_{\text{Ue}}(r) = -\frac{2\alpha Z\alpha}{3r} \int_0^\infty dr' r' \rho(r') \left[\chi_2(2|r-r'|) - \chi_2(2|r+r'|) \right]$$

$$\chi_n(z) = \int_1^\infty dt \exp(-tz) \frac{1}{t^n} \left(1 + \frac{1}{2t^2} \right) \sqrt{1 - \frac{1}{t^2}}$$

$$V_{\text{Ue}}(r) = V_{\text{point}}(r) \left[\frac{2\alpha}{3\pi} \chi_1(2r) \right]$$

Leading QED: Uehling



$$V_{\text{Ue}}(r) = -\frac{2\alpha Z\alpha}{3r} \int_0^\infty dr' r' \rho(r') \left[\chi_2(2|r-r'|) - \chi_2(2|r+r'|) \right]$$

$$\chi_n(z) = \int_1^\infty dt \exp(-tz) \frac{1}{t^n} \left(1 + \frac{1}{2t^2} \right) \sqrt{1 - \frac{1}{t^2}}$$

$$V_{\text{Ue}}(r) = V_{\text{point}}(r) \left[\frac{2\alpha}{3\pi} \chi_1(2r) \right]$$

$$V_{\text{Ue}}(r) \approx V_{\text{Fermi}}(r) \left[\frac{2\alpha}{3\pi} \chi_1(2r) \right]$$

Leading QED: Uehling

$V_{\text{Ue}}(r) = -\frac{2\alpha Z\alpha}{3r} \int_0^\infty dr' r' \rho(r') \left[\chi_2(2|r-r'|) - \chi_2(2|r+r'|) \right]$

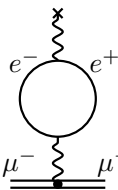
$$\chi_n(z) = \int_1^\infty dt \exp(-tz) \frac{1}{t^n} \left(1 + \frac{1}{2t^2} \right) \sqrt{1 - \frac{1}{t^2}}$$

$$V_{\text{Ue}}(r) = V_{\text{point}}(r) \left[\frac{2\alpha}{3\pi} \chi_1(2r) \right]$$

$$V_{\text{Ue}}(r) \approx V_{\text{Fermi}}(r) \left[\frac{2\alpha}{3\pi} \chi_1(2r) \right]$$

- accurate on the level of 0.2%
- $\Delta E_{\text{Ue}} \approx 70 \text{ keV}$

Leading QED: Uehling

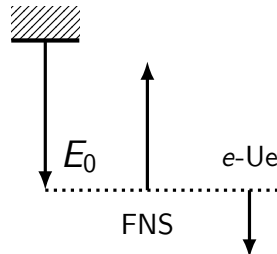


$$V_{\text{Ue}}(r) = -\frac{2\alpha Z\alpha}{3r} \int_0^\infty dr' r' \rho(r') \left[\chi_2(2|r-r'|) - \chi_2(2|r+r'|) \right]$$

$$\chi_n(z) = \int_1^\infty dt \exp(-tz) \frac{1}{t^n} \left(1 + \frac{1}{2t^2} \right) \sqrt{1 - \frac{1}{t^2}}$$

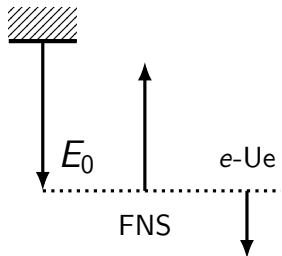
$$V_{\text{Ue}}(r) = V_{\text{point}}(r) \left[\frac{2\alpha}{3\pi} \chi_1(2r) \right]$$

$$V_{\text{Ue}}(r) \approx V_{\text{Fermi}}(r) \left[\frac{2\alpha}{3\pi} \chi_1(2r) \right]$$



- accurate on the level of 0.2%
- $\Delta E_{\text{Ue}} \approx 70 \text{ keV}$

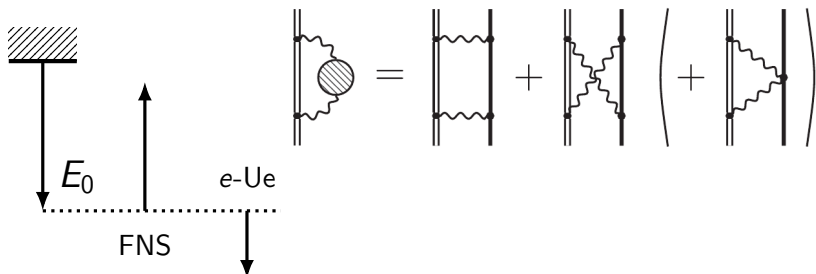
Sub-leading QED effects: nuclear polarization



Improvements:

Valuev *et al.*, PRL **128** 203001 (2022)

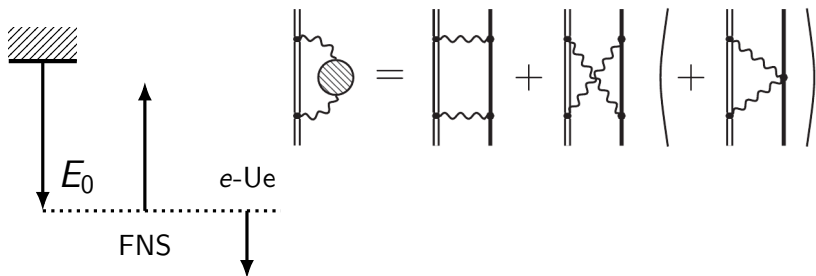
Sub-leading QED effects: nuclear polarization



Improvements:

Valuev *et al.*, PRL 128 203001 (2022)

Sub-leading QED effects: nuclear polarization

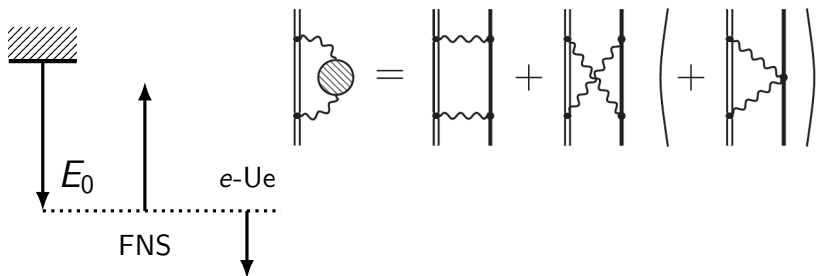


Improvements:

- field-theory approach, including transverse part
- state-of-art muonic and nuclear input, model dependence

Valuev *et al.*, PRL 128 203001 (2022)

Sub-leading QED effects: nuclear polarization

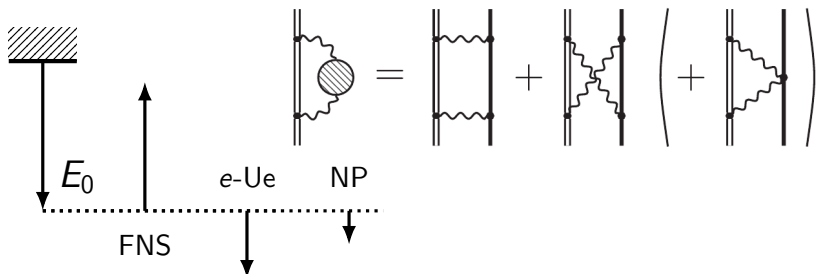


Improvements:

- field-theory approach, including transverse part
- state-of-art muonic and nuclear input, model dependence
- $0^+, 1^-, 2^+, 3^-, 4^+, 5^-$ and 1^+ excitation modes

Valuev *et al.*, PRL 128 203001 (2022)

Sub-leading QED effects: nuclear polarization

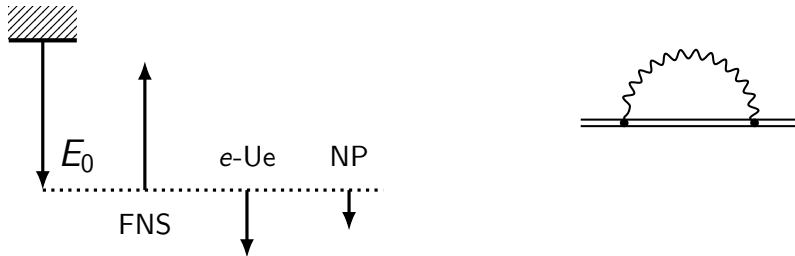


Improvements:

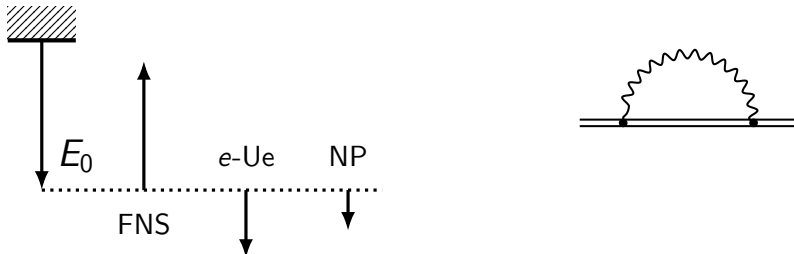
- field-theory approach, including transverse part
- state-of-art muonic and nuclear input, model dependence
- $0^+, 1^-, 2^+, 3^-, 4^+, 5^-$ and 1^+ excitation modes
- $4252 \text{ eV} \rightarrow 5712 \text{ eV}$

Valuev *et al.*, PRL **128** 203001 (2022)

Sub-leading QED effects: self energy and recoil



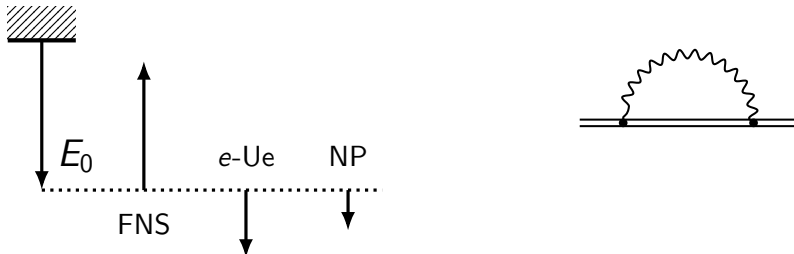
Sub-leading QED effects: self energy and recoil



Improvements SE and recoil:

- rigorous QED calculations

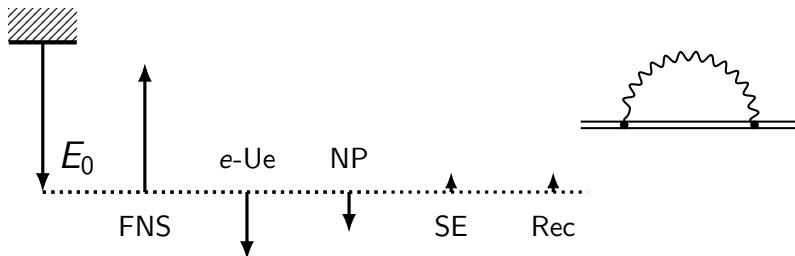
Sub-leading QED effects: self energy and recoil



Improvements SE and recoil:

- rigorous QED calculations
- SE: 2 methods, few grids and nuclear models

Sub-leading QED effects: self energy and recoil



Improvements SE and recoil:

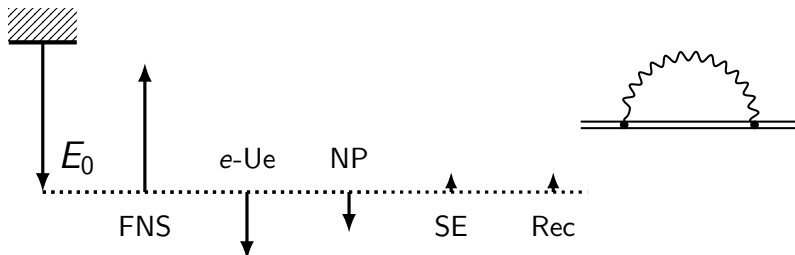
- rigorous QED calculations
- SE: 2 methods, few grids and nuclear models
- $\Delta E_{\text{SE}} = 3270(160)^{[1]}, 3373^{[2]} \text{ eV} \rightarrow 3225(15)^{[3]} \text{ eV}$

[1] Cheng *et al.*, PRA **17**, 489 (1978)

[2] Haga *et al.*, PRC **75**, 044315 (2007)

[3] Oreshkina, PRR **4**, L042040 (2022)

Sub-leading QED effects: self energy and recoil



Improvements SE and recoil:

- rigorous QED calculations
- SE: 2 methods, few grids and nuclear models
- $\Delta E_{\text{SE}} = 3270(160)^{[1]}, 3373^{[2]} \text{ eV} \rightarrow 3225(15)^{[3]} \text{ eV}$
- $\Delta E_{\text{rec}} = 385^{[4]*} \text{ eV} \rightarrow 3902^{[5]} \text{ eV}$

[1] Cheng *et al.*, PRA **17**, 489 (1978)

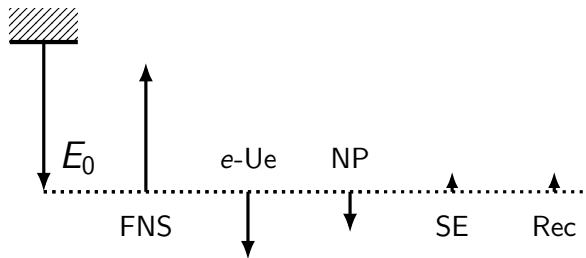
[2] Haga *et al.*, PRC **75**, 044315 (2007)

[3] Oreshkina, PRR **4**, L042040 (2022)

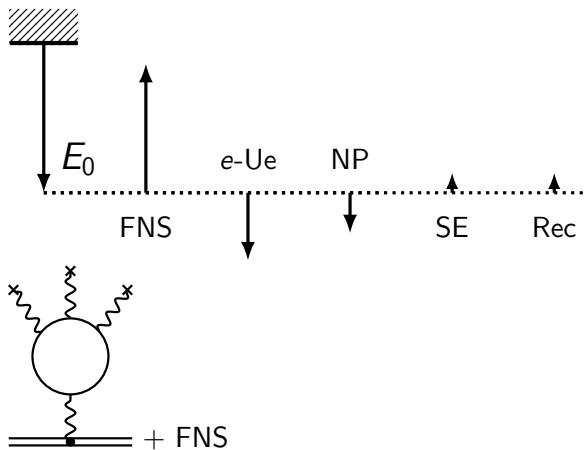
[4] Bergem *et al.*, PRC **37**, 2821 (1988)

[5] Yerokhin and Oreshkina, PRA **108**, 052824 (2023)

Sub-leading QED effects: Wichmann-Kroll, hadronic Ue

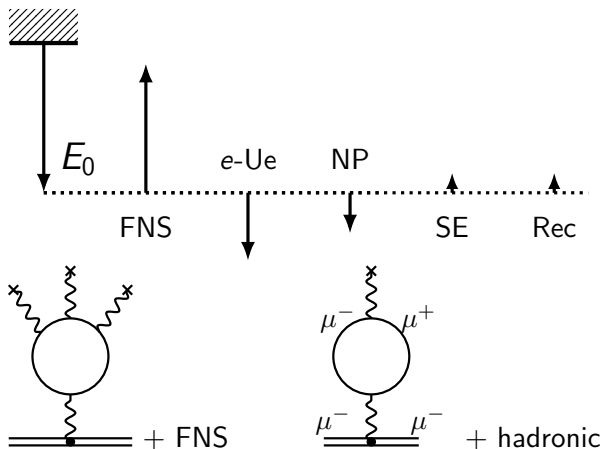


Sub-leading QED effects: Wichmann-Kroll, hadronic Ue



Sun, Mandrykina Oreshkina in preparation

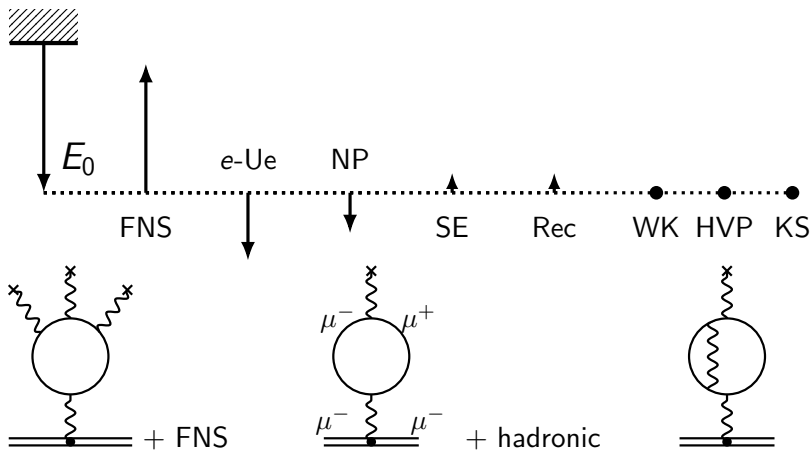
Sub-leading QED effects: Wichmann-Kroll, hadronic Ue



Sun, Mandrykina Oreshkina in preparation

Thierfeld, Mandrykina Oreshkina in preparation

Sub-leading QED effects: Wichmann-Kroll, hadronic Ue



Sun, Mandrykina Oreshkina in preparation

Thierfeld, Mandrykina Oreshkina in preparation

Muonic atoms' feature: dynamical structure, in ^{238}U

$$E_0 = 0 \text{ keV}$$

$$E_2 = 45 \text{ keV}$$

$$E_4 = 150 \text{ keV}$$

Muonic atoms' feature: dynamical structure, in ^{238}U

$$E_0 = 0 \text{ keV}$$

$$E_2 = 45 \text{ keV}$$

$$E_4 = 150 \text{ keV}$$

$$\Delta E_{2p} = 220 \text{ keV}$$

Muonic atoms' feature: dynamical structure, in ^{238}U

$$E_0 = 0 \text{ keV}$$

$$E_2 = 45 \text{ keV}$$

$$E_4 = 150 \text{ keV}$$

$$\Delta E_{2p} = 220 \text{ keV}$$

$$I(0, 2, 4) + \mu^-(2p_{1/2}, 2p_{3/2})$$

Muonic atoms' feature: dynamical structure, in ^{238}U

$$E_0 = 0 \text{ keV}$$

$$E_2 = 45 \text{ keV}$$

$$E_4 = 150 \text{ keV}$$

$$\Delta E_{2p} = 220 \text{ keV}$$

$$I(0, 2, 4) + \mu^-(2p_{1/2}, 2p_{3/2})$$

$$F = 1/2 \quad \boxed{} \quad \boxed{}$$

$$3/2 \quad \boxed{} \quad \boxed{} \quad \boxed{}$$

$$5/2 \quad \boxed{} \quad \boxed{} \quad \boxed{}$$

$$7/2 \quad \boxed{} \quad \boxed{} \quad \boxed{}$$

$$9/2 \quad \boxed{} \quad \boxed{}$$

$$11/2 \quad \boxed{}$$

Muonic atoms' feature: dynamical structure, in ^{238}U

$$E_0 = 0 \text{ keV}$$

$$E_2 = 45 \text{ keV}$$

$$E_4 = 150 \text{ keV}$$

$$\Delta E_{2p} = 220 \text{ keV}$$

$$I(0, 2, 4) + \mu^-(2p_{1/2}, 2p_{3/2})$$

$$F = 1/2 \quad \boxed{} \quad \boxed{}$$

$$3/2 \quad \boxed{} \quad \boxed{} \quad \boxed{}$$

$$5/2 \quad \boxed{} \quad \boxed{} \quad \boxed{}$$

$$7/2 \quad \boxed{} \quad \boxed{} \quad \boxed{}$$

$$9/2 \quad \boxed{} \quad \boxed{}$$

$$11/2 \quad \boxed{}$$

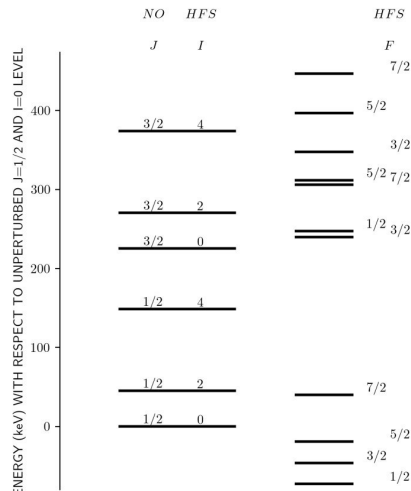


Fig: Zoia Mandrykina

Results for ^{208}Pb RMS extraction PRELIMINARY

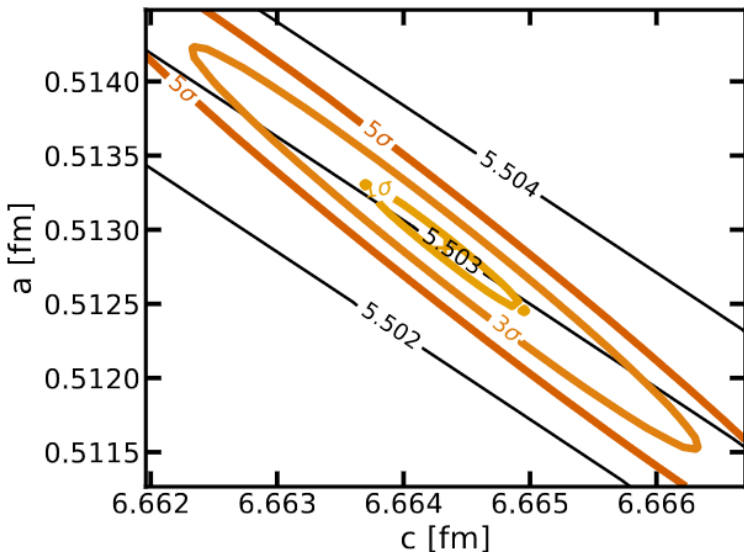
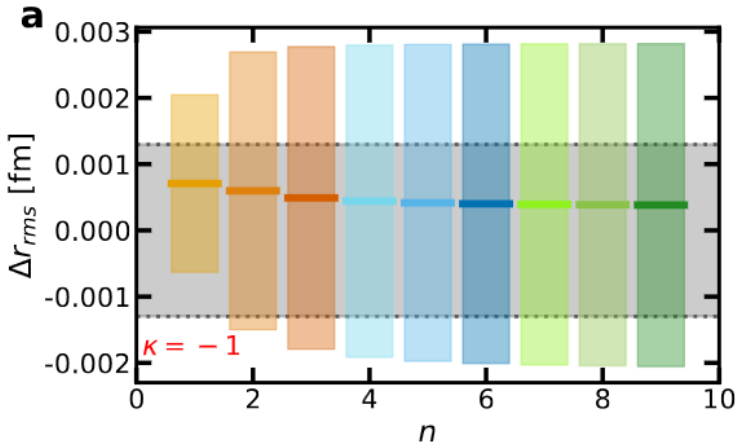


Fig: Konstantin Beyer

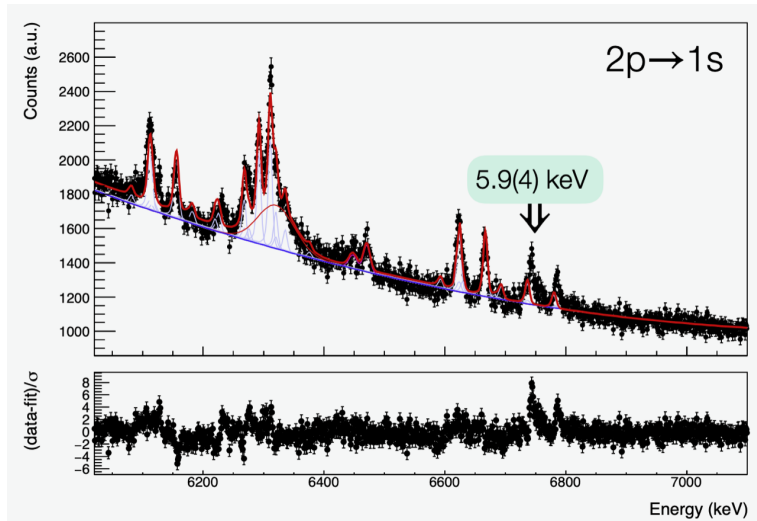
Model dependence PRELIMINARY



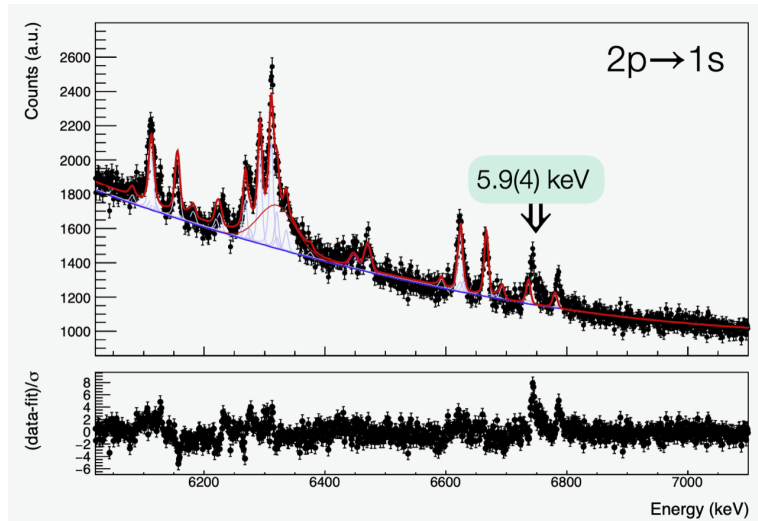
The difference between the Fermi-equivalent radius and the tabulated value. The solid colourful line is the mean value over all SKYRME distributions.

Fig: Konstantin Beyer

Ongoing analysis of $2p - 1s$ in ^{248}Cm PRELIMINARY



Ongoing analysis of $2p - 1s$ in ^{248}Cm PRELIMINARY



same problems: some lines are off \Rightarrow no accurate RMS
could be connected with other cases (Zr, Sn, Pb)

Summary

- Muonic atom: QED for “heavy electron”
- Probe of nuclear parameters and new approaches

Yerokhin and Oreshkina, PRA **108**, 052824 (2023)

N. S. Oreshkina, PRR **4**, L042040 (2022)

I. A. Valuev, G. Colò, X. Roca-Maza, C. H. Keitel, and N. S. Oreshkina, PRL **128**, 203001 (2022)

A. Antognini *et al.*, PRC **101**, 054313 (2020)

Summary

- Muonic atom: QED for “heavy electron”
- Probe of nuclear parameters and new approaches
- State-of-the-art theory predictions including refined NP, SE and recoil values

Yerokhin and Oreshkina, PRA **108**, 052824 (2023)

N. S. Oreshkina, PRR **4**, L042040 (2022)

I. A. Valuev, G. Colò, X. Roca-Maza, C. H. Keitel, and N. S. Oreshkina, PRL **128**, 203001 (2022)

A. Antognini *et al.*, PRC **101**, 054313 (2020)

Summary

- Muonic atom: QED for “heavy electron”
- Probe of nuclear parameters and new approaches
- State-of-the-art theory predictions including refined NP, SE and recoil values
- Re-evaluation of RMS is needed



Find an elephant

Yerokhin and Oreshkina, PRA **108**, 052824 (2023)

N. S. Oreshkina, PRR **4**, L042040 (2022)

I. A. Valuev, G. Colò, X. Roca-Maza, C. H. Keitel, and N. S. Oreshkina, PRL **128**, 203001 (2022)

A. Antognini *et al.*, PRC **101**, 054313 (2020)

Acknowledgments to the hard-working team

Zewen Sun, Zoya Mandrykina, Moritz Theirlfeld, Igor A. Valuev,
Niklas Michel, Konstantin Beyer (MPIK)
Gianluca Colò, Xavier Roca-Maza (INFN Milano)
Stella Vogiatzi, Andreas Knecht (PSI) and muX collaboration



Image: Barge Haulers on the Volga by Ilya Repin

Acknowledgments to the hard-working team

Zewen Sun, Zoya Mandrykina, Moritz Theirlfeld, Igor A. Valuev,
Niklas Michel, Konstantin Beyer (MPIK)
Gianluca Colò, Xavier Roca-Maza (INFN Milano)
Stella Vogiatzi, Andreas Knecht (PSI) and muX collaboration

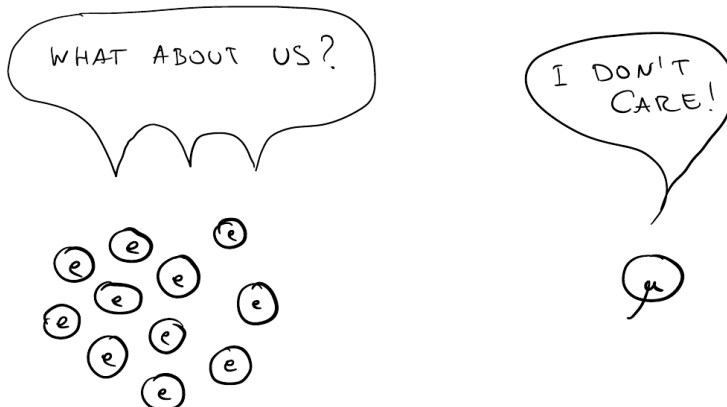


Image: Barge Haulers on the Volga by Ilya Repin

Thank you for your attention

A frequently asked question:

What's about electrons correlation and electron-muon interaction?



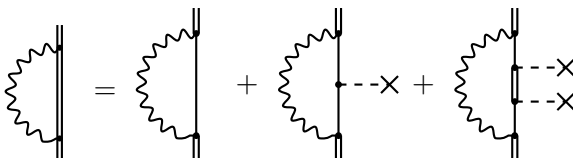
Two leptons \Rightarrow 1s for muons and 1s for electrons

- Electrons are far
- The electron screening effect has been calculated and negligible

Self-energy correction

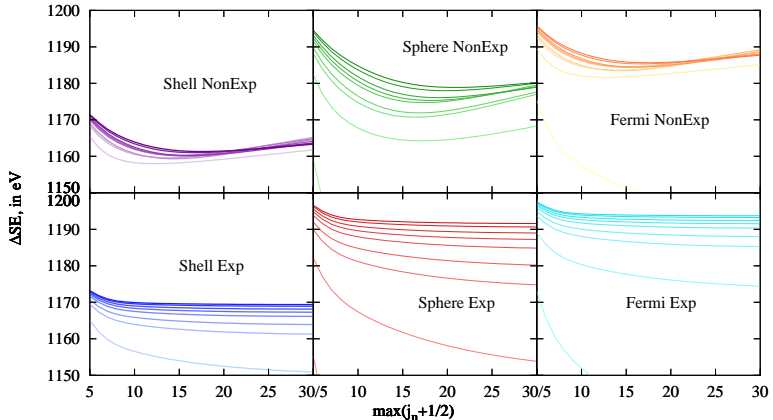
$$\langle a | \Sigma(E) | b \rangle = \frac{i}{2\pi} \int_{-\infty}^{\infty} d\omega \sum_n \frac{\langle an | I(\omega) | nb \rangle}{E - \omega - \varepsilon_n(1 - i0)},$$

$$I(\omega, \mathbf{x}_1, \mathbf{x}_2) = \frac{(1 - \alpha_1 \alpha_2) \exp(i\sqrt{\omega^2 + i0}x_{12})}{4\pi x_{12}}.$$



- 0pot, 1pot: momentum representation
- Many-pot: coordinate representation, partial waves expansion
- Contains infinite summation over intermediate κ
- Three nuclear models: shell, sphere, Fermi
- Two integration grids

Models and grid compared: $\mu - {}^{90}_{40}\text{Zr}$



ΔE_{SE} contribution to the $1s_{1/2}$ state of the muonic zirconium in units of eV as a function of maximal intermediate angular momentum j_n for different nuclear models and numerical grids. The colors of the lines on every panel change depending on the number of used DKB basis functions from light for $n_{\text{DKB}} = 50$ to dark for $n_{\text{DKB}} = 150$

SE: results

Ion	State	Final	Previous	[Haga <i>et al.</i> , PRC 75 , 044315 (2007)]
$\mu - {}^{90}\text{Zr}$	$1s_{1/2}$	1191(4)	1218	
	$2p_{1/2}$	6.99(5)	1	
	$2p_{3/2}$	46.52(6)	41	
	$\Delta 2p$	39.53(8)	40	
$\mu - {}^{208}\text{Pb}$	$1s_{1/2}$	3225(15)	3373	
			3270(160)*	[Cheng <i>et al.</i> , PRA 17 , 489 (1978)]
	$2p_{1/2}$	453(5)	413	
	$2p_{3/2}$	745(5)	707	
	$\Delta 2p$	292(7)	294	

- Order-of-magnitude improvement for $1s_{1/2}$ state
- First rigorous predictions for $2p_{1/2}$, $2p_{3/2}$

Transverse part of muon-nucleus interaction

$$H = H_N + \alpha \mathbf{p} + \beta m_\mu + V(\mathbf{r}, \mathbf{r}_{N_i})$$

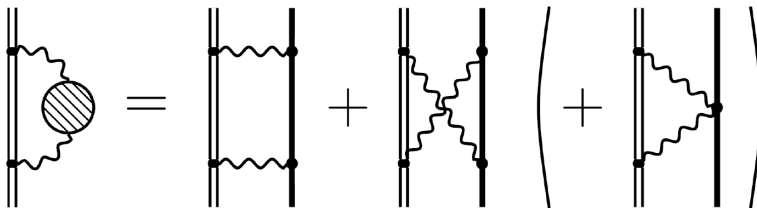


$$H = H_N + \alpha(\mathbf{p} - e\mathbf{A}(\mathbf{r}, \mathbf{r}_{N_i})) + \beta m_\mu + V(\mathbf{r}, \mathbf{r}_{N_i})$$

- Longitudinal (or Coulomb) interaction $V(\mathbf{r}, \mathbf{r}_{N_i})$
always $|\Delta E_{2p_1/2}^{\text{NP}}| > |\Delta E_{2p_3/2}^{\text{NP}}|$
- Transverse interaction $\mathbf{A}(\mathbf{r}, \mathbf{r}_{N_i})$
contributes with the opposite muon-spin dependence
- However, the anomalies still persisted (for more than 40 years)

Tanaka and Horikawa, Nucl. Phys. **A580**, 291 (1994)

Total leading-order nuclear polarization



$$\Delta E_{\text{NP}}^{\text{L}} = -i(4\pi\alpha)^2 \sum_{i'I'} \iint \frac{d\mathbf{q} d\mathbf{q}'}{(2\pi)^6} \int \frac{d\omega}{2\pi} \frac{D_{\mu\xi}(\omega, \mathbf{q}) D_{\zeta\nu}(\omega, \mathbf{q}') \langle iI | j_m^\mu(-\mathbf{q}) J_N^\xi(\mathbf{q}) | i'I' \rangle \langle i'I' | J_N^\zeta(-\mathbf{q}') j_m^\nu(\mathbf{q}') | iI' \rangle}{(\omega + \omega_m - iE_{i'}\epsilon)(\omega - \omega_N + i\epsilon)},$$

$$\Delta E_{\text{NP}}^{\text{X}} = +i(4\pi\alpha)^2 \sum_{i'I'} \iint \frac{d\mathbf{q} d\mathbf{q}'}{(2\pi)^6} \int \frac{d\omega}{2\pi} \frac{D_{\mu\xi}(\omega, \mathbf{q}) D_{\zeta\nu}(\omega, \mathbf{q}') \langle iI' | j_m^\mu(-\mathbf{q}) J_N^\xi(\mathbf{q}) | i'I \rangle \langle i'I | J_N^\zeta(-\mathbf{q}') j_m^\nu(\mathbf{q}') | iI' \rangle}{(\omega + \omega_m - iE_{i'}\epsilon)(\omega + \omega_N - i\epsilon)},$$

$$\Delta E_{\text{NP}}^{\text{SG}} = -i(4\pi\alpha)^2 \sum_i \iint \frac{d\mathbf{q} d\mathbf{q}'}{(2\pi)^6} \int \frac{d\omega}{2\pi} \frac{D_{\mu\xi}(\omega, \mathbf{q}) \delta^{\xi\zeta} D_{\zeta\nu}(\omega, \mathbf{q}') \langle i | j_m^\mu(-\mathbf{q}) | i' \rangle \langle i' | j_m^\nu(\mathbf{q}') | i \rangle \langle I | \rho_N(\mathbf{q} - \mathbf{q}') | I \rangle}{(\omega + \omega_m - iE_{i'}\epsilon)} \frac{m_p}{m_p},$$

summations over entire muonic (i') and nuclear (I') spectra

Muonic spectrum

Dirac equation:

$$[\alpha \mathbf{p} + \beta m_\mu + V_0(\mathbf{r})]\psi(\mathbf{r}) = E\psi(\mathbf{r})$$

V_0 from Fermi nuclear charge distribution

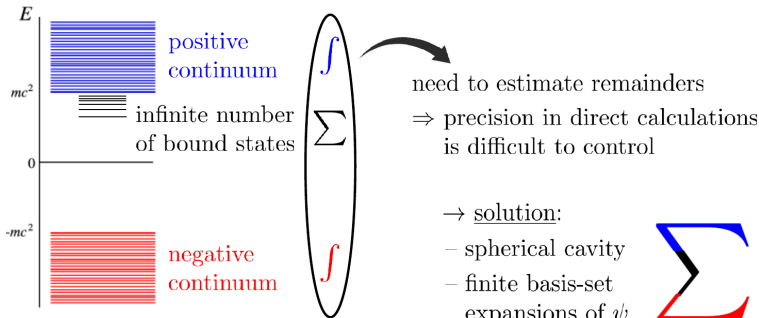


Fig: Igor Valuev

Skyrme-type nuclear interaction



Tony Skyrme in 1946

Fig:

[https://en.wikipedia.org/
wiki/Tony_Skyrme](https://en.wikipedia.org/wiki/Tony_Skyrme)

$$\begin{aligned}
 V(\mathbf{r}_1, \mathbf{r}_2) = & t_0(1 + \chi_0 P_\sigma)\delta(\mathbf{r}) \\
 & + \frac{1}{2}t_1(1 + \chi_1 P_\sigma)[\mathbf{P}^{\dagger 2}\delta(\mathbf{r}) + \delta(\mathbf{r})\mathbf{P}^2] \\
 & + t_2(1 + \chi_2 P_\sigma)\mathbf{P}^\dagger \cdot \delta(\mathbf{r})\mathbf{P} \\
 & + \frac{1}{6}t_3(1 + \chi_3 P_\sigma)\rho^\lambda(\mathbf{R})\delta(\mathbf{r}) \\
 & + iW_0(\boldsymbol{\sigma}_1 + \boldsymbol{\sigma}_2) \cdot [\mathbf{P}^\dagger \times \delta(\mathbf{r})\mathbf{P}]
 \end{aligned}$$

$$\mathbf{r} = \mathbf{r}_1 - \mathbf{r}_2, \mathbf{R} = \frac{1}{2}(\mathbf{r}_1 + \mathbf{r}_2)$$

$$\mathbf{P} = \frac{1}{2i}(\nabla_1 - \nabla_2), P_\sigma = \frac{1}{2}(1 + \boldsymbol{\sigma}_1 \cdot \boldsymbol{\sigma}_2)$$

10 parameters
Nuclear wave functions
dependence

Nuclear spectrum

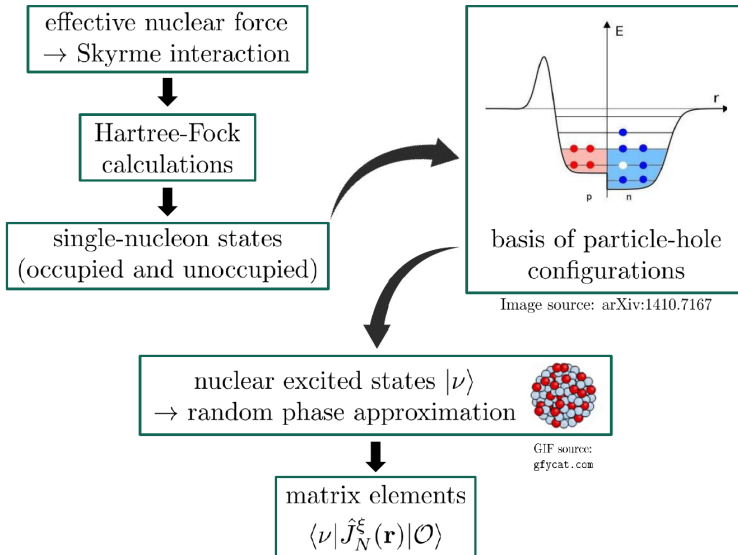
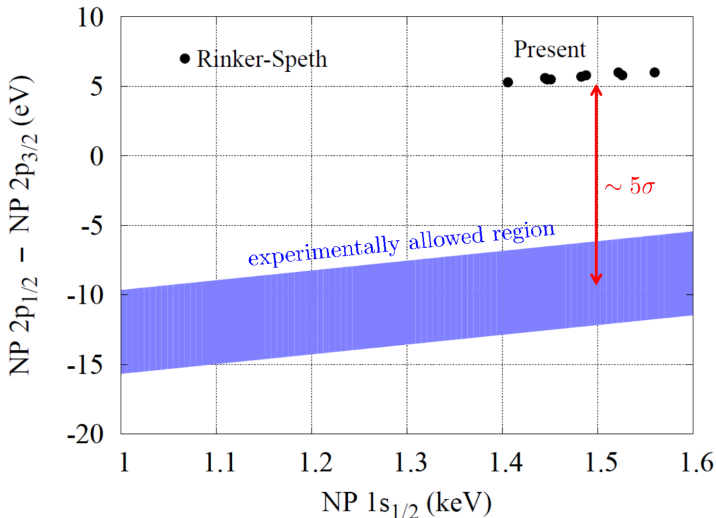


Fig: Igor Valuev

Calculations details

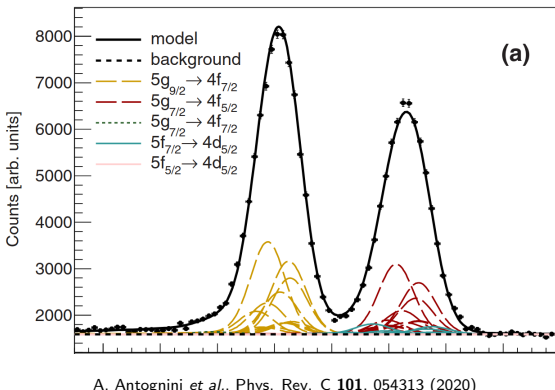
- rigorous QFT approach
- Feynman and Coulomb gauges
- complete muonic Dirac spectrum
- 9 different parametrizations of the Skyrme interaction
- Covers all realistic ranges for nuclear properties
- $0^+, 1^-, 2^+, 3^-, 4^+, 5^-$ and 1^+ excitation modes
- RMS value changes the NP predictions
- Comparison between theory and free-parameter fit of the experimental data

Nuclear polarization correction ^{90}Zr



around 15 eV (5σ) gap remains practically constant

Comparison with experimental spectra $5g \rightarrow 4f$



A. Antognini *et al.*, Phys. Rev. C **101**, 054313 (2020)

$$Q[185] = 2.07(5) \text{ b}, Q[187] = 1.94(5) \text{ b}$$

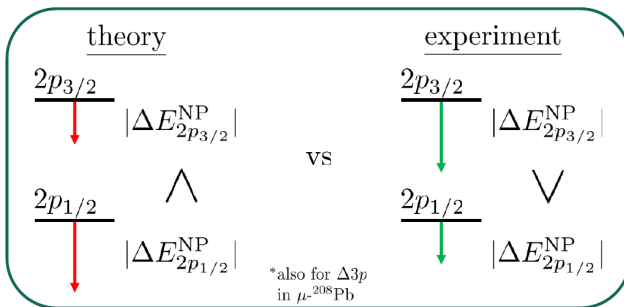
Analysis of $2p \rightarrow 1s$ would give rms value

But!

A fine-structure anomaly

muonic ^{90}Zr , $^{112-124}\text{Sn}$, ^{208}Pb : very poor fit, $\chi^2/\text{DF} = 187$

→ nuclear polarization correction as variable parameters
 → the root of the problem



$2p_{1/2}$ is closer to a nucleus and should be affected more strongly

P. Bergem *et al.*, Phys. Rev. C 37 2821 (1988)

Nuclear polarization effect

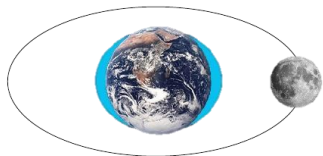


Image source: www.universetoday.com

$$V_{NP}(r) = -\alpha \sum_Z \frac{1}{|\mathbf{r} - \mathbf{r}_{N_i}|}$$

$$\Delta E_{NP} = \sum_{nN} \frac{|\langle aA | \delta V | nN \rangle|^2}{E_{aA} - E_{nN}}$$

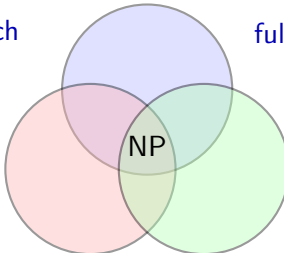
Longitudinal (Coulomb) part

Transverse part: $H = H_N + \alpha(\mathbf{p} - e\mathbf{A}(\mathbf{r}, \mathbf{r}_{N_i})) + \beta m_\mu + V(\mathbf{r}, \mathbf{r}_{N_i})$

field-theory approach

full muon-nucleus interaction

precise
muonic
description

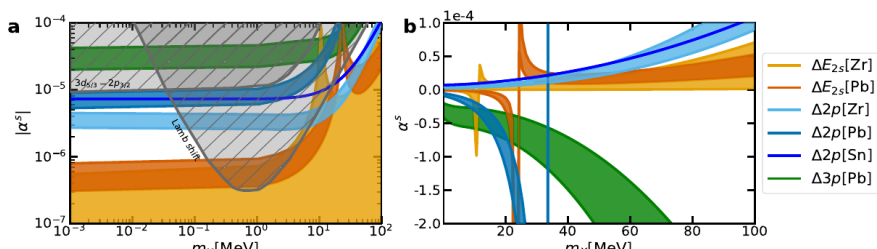


state-of-art
nuclear input

Alternative explanations

~~Exploring New Solutions to the Fine Structure Anomaly in Heavy Muonic Atoms~~

How not to solve the Fine-Structure Anomaly in Heavy Muonic Atoms



**MAX PLANCK
GESELLSCHAFT**

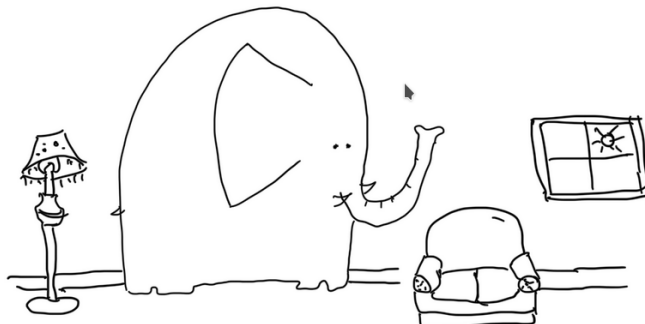


MAX-PLANCK-INSTITUT
FÜR KERNPHYSIK

Status of theory for heavy muonic atoms

An elephant in the room

- RMS: high importance
- From muonic spectra
- High accuracy:
0.02% for lead
- Fine-structure anomaly
- Poor fit $\chi^2/\text{DF} = 187$
- Estimation for theory
- How much can we trust it?...



FIND AN ELEPHANT

NSO